Current Research (2015) Newfoundland and Labrador Department of Natural Resources Geological Survey, Report 15-1, pages 105-123

NEW U–Pb AGE CONSTRAINTS ON THE DEVELOPMENT OF URANIUM MINERALIZATION WITHIN THE CENTRAL MINERAL BELT OF LABRADOR

G.W. Sparkes and G.R. Dunning[1]
Mineral Deposits Section
[1]Department of Earth Sciences, Memorial University, St. John's, NL, A1B 3X5

ABSTRACT

*New geochronological data provide further insight(s) into the timing of uranium mineralization within the Central Mineral Belt (CMB) of Labrador, and allows for the modification of existing models regarding geological development and metallogenic events. Ongoing investigations are aimed at establishing a better understanding of the various styles of uranium mineralization, and providing better constraints with respect to the timing of uranium enrichment. Several new U–Pb results provide absolute or relative age constraints on the formation of uranium mineralization. Archean basement rocks of the Nain Province, which host the Two Time uranium deposit, gave an age of 3043 ± 2.5 Ma, providing a maximum limit on the development of uranium mineralization in that area. At the Kitts deposit, the Kitts metagabbro unit of the Post Hill Group gave an age of 2018 +15/-8 Ma, providing a maximum age for mineralization. The host rock at the largest uranium deposit in the region, the Michelin deposit, gave an age of 1858 ± 2 Ma, providing a maximum age on the development of uranium mineralization, and confirming that the mineralizing event is younger than that at Kitts, which is constrained by a previously reported minimum age of 1882 Ma. Titanite data from the dated sample at Michelin provide evidence for a complex and protracted thermal history, which include events of Labradorian (*ca. *1650 Ma) and Grenvillian (*ca. *1000 Ma) age. Finally, several undeformed intrusive units in the area of the Jacques Lake and Michelin deposits produced ages of 1798 ± 2 Ma and 1644 ± 4 Ma, respectively. These data, combined with previously published geochronology, support at least three different uranium mineralizing events within the CMB. These events occurred between 2030 and 1880 Ma, between 1860 and 1800 Ma, and later than 1650 Ma.*

INTRODUCTION

The Central Mineral Belt (CMB) of Labrador is a well-known uranium province (*cf.,* Beavan, 1958; Gandhi, 1978; Gower *et al.*, 1982; Ryan, 1984; Wilton, 1996; Sparkes and Kerr, 2008). Within the CMB, uranium mineralization displays considerable variation in both host rock and style. The rocks hosting uranium mineralization within the CMB range in age from Archean to late Paleoproterozoic. Ongoing investigations into the genesis of uranium mineralization in the region are aimed at providing a better understanding of the distribution, style and timing of the various mineralizing events, and a regional compilation report is in preparation. The U–Pb geochronology is an important part of this work, and provides relative age constraints on the formation of select mineralizing events. Earlier reports, which were focused in the eastern portion of the CMB, provided some constraints in relation to the development of specific deposits; these include the minimum age of 1881 ± 3.4 Ma for the Kitts deposit (Sparkes *et al*., 2010), and the minimum age of 1801 ± 0.9 Ma for the Jacques Lake deposit (Sparkes and Dunning, 2009). New data, coupled with existing geochronology for the region, now provide evidence for at least three separate mineralizing events that can be broadly grouped as 2030 to 1880 Ma, 1860 to 1800, and post 1650 Ma.

New U–Pb data presented herein include ages produced from zircon, titanite and monazite, all of which were obtained from selected samples collected in the vicinity of known uranium deposits. Several of these new ages provide supporting evidence for volcanic and plutonic events already identified within the region, but others identify previously unrecognized events that have yet to be completely defined. To date, most of this sampling has been concentrated in the eastern portion of the CMB, as rocks in the western portion of the belt, which have relevance to uranium mineralization, are generally not suitable for U–Pb geochronology. This report presents U–Pb geochronological data from several deposits, and discusses these in the context of earlier findings.

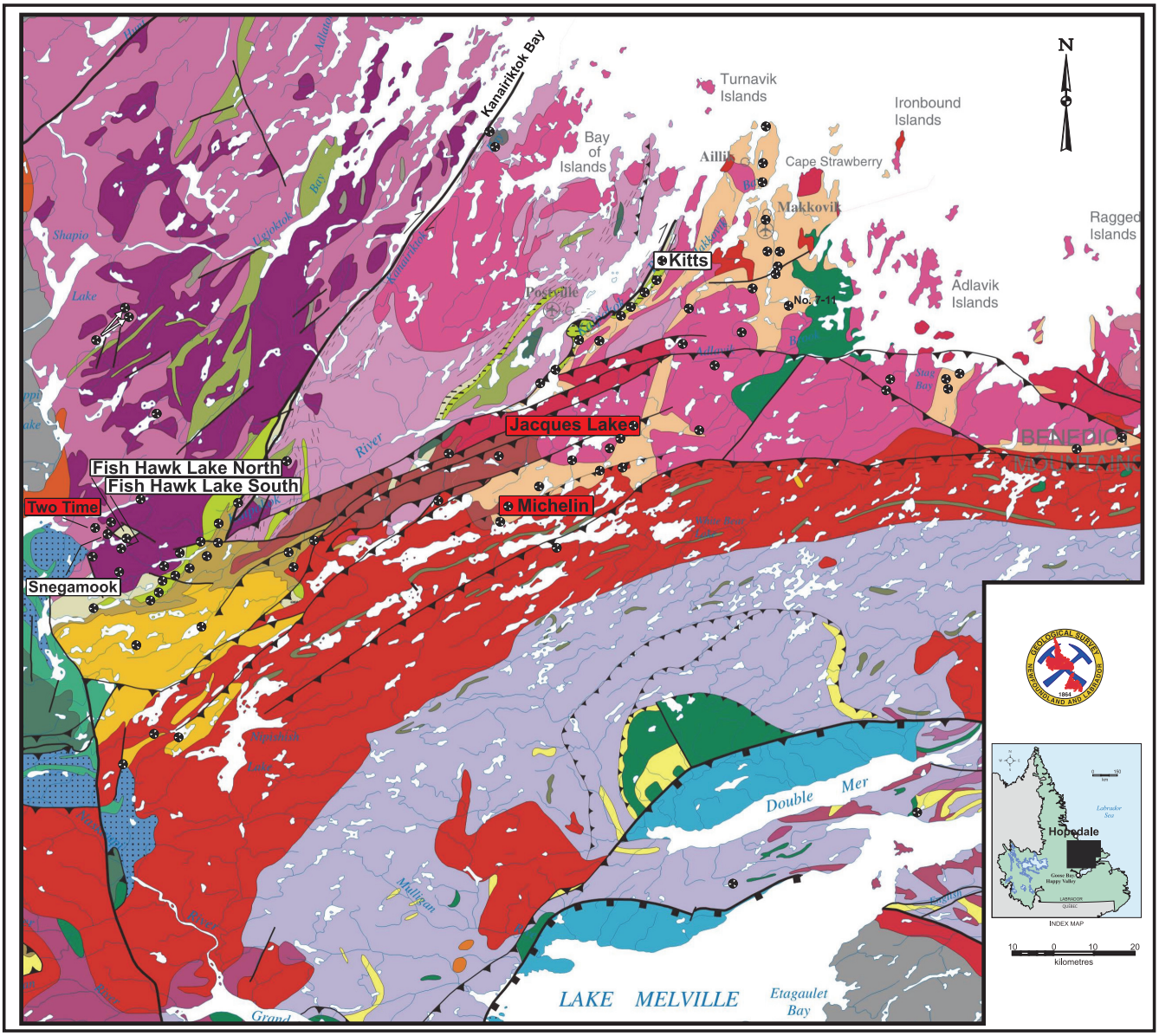

Figure 1. *Geological map of the Central Mineral Belt and surrounding region outlining select uranium occurrences; those highlighted in red contain defined NI43-101 resources. Geological base map modified from Wardle* et al. *(1997).*

REGIONAL GEOLOGY

The CMB of Labrador (Figure 1) spans several different structural provinces including portions of the Archean Nain Province to the north, the Paleoproterozoic Makkovik and Churchill provinces in the eastern and western portions, and the Mesoproterozoic Grenville Province to the south. The CMB has no firm geological boundaries, rather it is largely defined on the basis of the distribution of mineralization. Uranium is the most abundant commodity, but there is also Cu, Mo and REE. The regional geology of the area encompassed by the CMB has been summarized by Bailey (1979), Gower *et al*. (1982), Ryan (1984), Ermanovics (1993), Kerr (1994), Kerr *et al*. (1996), Wilton (1996), Hinchey (2007) and Hinchey and LaFlamme (2009); the following summary is largely derived from these sources.

Rocks within the Archean Nain Province and their reworked equivalents represent the oldest units in the region, and form the basement rocks to the Proterozoic supracrustal sequences (Ryan, 1984; Ermanovics, 1993; Kerr *et al*., 1996). The rocks of the Nain Province consist of orthogneiss, commonly referred to as Maggo gneiss, along with lesser remnants of an older supracrustal sequence referred to as the Weekes amphibolite (Ermanovics, 1993). The Maggo gneiss produced a U–Pb zircon age of 3105 +6/-

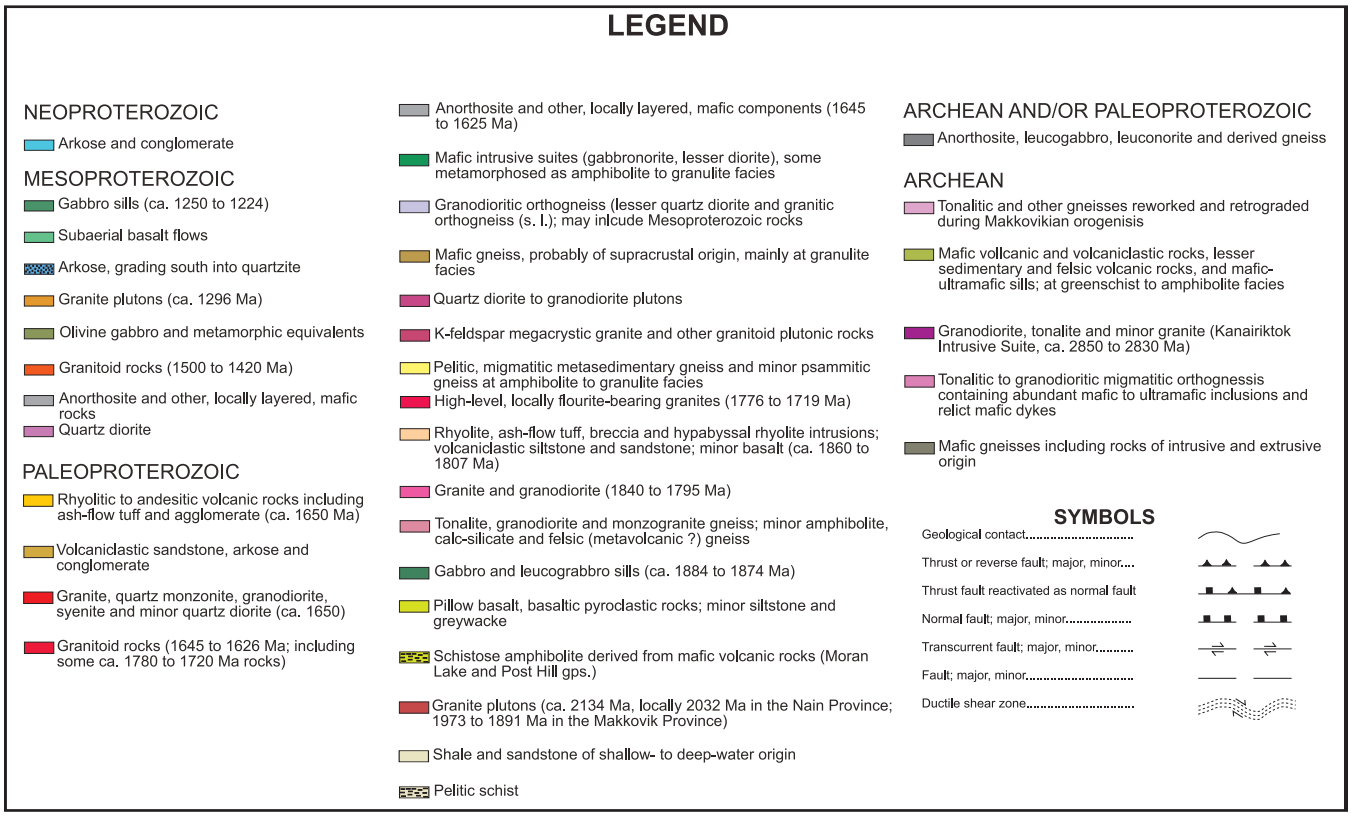

Figure 1. *Geological map of the Central Mineral Belt and surrounding region outlining select uranium occurrences; those highlighted in red contain defined NI43-101 resources. Geological base map modified from Wardle* et al. *(1997).*

9 Ma, which was interpreted as a tentative emplacement age for the precursor of the gneissic unit (Loveridge *et al*., 1987). The orthogneiss is intruded by rocks of the Kanairiktok intrusive suite, which consist of massive to strongly foliated tonalite, granodiorite and granite. A sample of tonalite from the Kanairiktok intrusive suite produced a U–Pb zircon age with an upper intercept of 2858 +4/-3 Ma (Loveridge *et al*., 1987). Both the orthogneiss and Kanairiktok intrusive suite are crosscut by a sequence of mafic dykes, known as the Kikkertavak dykes, which have been dated at 2235 ± 2 Ma (Cadman *et al*., 1993). These dykes do not crosscut the overlying supracrustal sequences of the CMB and therefore provide a maximum age constraint for the deposition of the Moran Lake and Post Hill groups.

In the western portion of the CMB, the Archean basement rocks are unconformably overlain by the siliciclastic sedimentary rocks of the Moran Lake Group (Smyth *et al.,* 1978; Wardle and Bailey, 1981; Ryan, 1984). The upper portion of the Moran Lake Group consists of pillow basalt, which hosts uranium mineralization (*e.g.*, Moran Lake C Zone deposit); these rocks have undergone greenschist-facies metamorphism. The Moran Lake Group is, in turn, unconformably overlain by the Bruce River Group (Ryan, 1984). The lower portion of this sequence is composed of terrestrial conglomerates, arkoses and sandstones, which are, in turn, overlain by a thick succession of predominantly subaerial felsic volcanic rocks, locally dated at 1649 ± 1Ma (Schärer *et al*., 1988).

In the eastern CMB, the Archean basement rocks, and their reworked equivalents, are tectonically overlain by supracrustal rocks of the Post Hill Group (Marten, 1977; Ketchum *et al*., 2002), which are inferred to be coeval with the Moran Lake Group (*cf*., Marten, 1977; Wardle and Bailey, 1981). The Post Hill Group is composed of psammite, schistose mafic metavolcanic rocks and minor pelite (Culshaw and Ketchum, 1995). The Post Hill Group is much more strongly deformed, largely at amphibolite facies. A tuff layer, within the lower portion of the Post Hill Group stratigraphy, produced a U–Pb zircon age of 2178 ± 4 Ma, which is interpreted to be the formational age of that unit (Ketchum *et al*., 2001). The metavolcanic rocks are, in turn, overlain by psammitic and semipelitic metasedimentary rocks that were deposited after 2013 Ma, based on detrital zircon contained within the unit (Ketchum *et al*., 2001). This sequence is overlain by metabasalt of the Kitts Pillow Lava, which is host to the high-grade Kitts uranium deposit, and represents the highest stratigraphic unit within the Post Hill Group (*cf*., Marten, 1977; Ketchum *et al*., 2002). In general terms, these

rocks are viewed as equivalents to the upper portions of the Moran Lake Group.

Sedimentary and metavolcanic rocks of the Aillik Group are in tectonic contact with the Post Hill Group. This sequence is composed of interbedded sandstone, siltstone, conglomerate, tuffaceous sandstone, felsic tuff, rhyolite, volcanic breccia and lesser mafic volcanic rocks and volcaniclastic sedimentary rocks (Hinchey and LaFlamme, 2009). Metavolcanic rocks within this group range in age from 1883 to 1856 Ma (*cf.*, Schärer *et al.,* 1988; Hinchey and Rayner, 2008). The sequence is also intruded by variably foliated granitoid rocks that can be broadly segregated into three main intrusive events, namely *ca.*1800 Ma, *ca.* 1720 Ma and *ca.* 1650 Ma (Kerr *et al*., 1992; Kerr, 1994).

The supracrustal rocks of the CMB are host to a variety of different styles of uranium mineralization; these have largely been grouped into three main categories: 1) magmatic, 2) metamorphic−metasomatic, and 3) sediment-hosted (Sparkes and Kerr, 2008). Under this broad subdivision no one style of mineralization is confined to a specific period of time within the CMB.

U–Pb GEOCHRONOLOGY

Results from six samples are discussed in this report. These include a sample of Archean basement rock that hosts the Two Time deposit, a sample from the Kitts metagabbro that forms the footwall to the Kitts deposit, and several supracrustal and intrusive units from the vicinity of the Michelin and Jacques Lake deposits. All samples were processed by standard techniques of crushing and concentration of heavy mineral separates consisting of zircon, monazite and titanite. Most titanite and all monazite were physically abraded following the procedure of Krogh (1982) and zircons were either physically or chemically abraded (*cf.*, Mattinson, 2005). Lead and uranium isotopic ratios were measured by thermal ionization mass spectrometry, and results calculated using ISOPLOT for weighted averages or following the procedure of Davis (1982) for linear regressions. Uncertainties on all ages are reported at the 95% confidence interval (2σ). The following summary provides a brief description of each unit and its corresponding age determination.

TWO TIME DEPOSIT

Uranium mineralization in the area of the Two Time deposit (Figure 1), and south along the Two Time Trend to the area of the Snegamook and Fish Hawk Lake prospects (Figure 2) is primarily hosted by a quartz monzodiorite−tonalite phase, inferred to be part of the regionally extensive Kanairiktok intrusive suite (Sparkes and Kerr, 2008; Ross, 2009). A sample of the quartz monzodiorite−tonalite host rock to the uranium mineralization was collected from drillcore at the Snegamook prospect (Sample #GS-09-44; DDH SN-08-08, 49 m depth); here the unit is locally less affected by the pervasive hematite alteration and associated cataclastic brecciation associated with the uranium mineralization. The sample consisted of relatively unaltered, medium-grained, quartz monzodiorite−tonalite (Plate 1), which as shown in Plate 2 is locally affected by hematite alteration and accompanying uranium mineralization. In thin section, the sample consists of interlocking plagioclase and quartz along with lesser chlorite and opaque minerals that are mostly developed along grain boundaries (Plate 3A, B). The sample yielded both zircon and monazite (Plate 4). Three analyses of euhedral zircon prisms that show excellent igneous growth zoning (Plate 5) yield triplicate concordant points and a weighted average $^{207}Pb/^{206}Pb$ age of 3043 ± 2.5 Ma (95% CI, MSWD = 0.18; Figure 3). In addition, three monazite analyses consisting of one or two grains each are concordant to discordant on a line that yields an upper intercept age of 2688 +6/-3 Ma (5% probability of fit), whereas the concordant point alone yields a $^{207}Pb/^{206}Pb$ age of 2689.7 ± 0.6 Ma (2 σ). The lower intercept of this line is *ca.* 1300 Ma, with a large uncertainty due to the length of the projection, but the data suggest that the rock may have been subject to a thermal event or disturbance at this time. The age of 3043 ± 2.5 Ma is interpreted as the crystallization age of the quartz monzodiorite−tonalite unit and provides a maximum age limit for the development of uranium mineralization along the Two Time Trend, whereas the monazite likely records a metamorphic overprint. The age is approximately 200 million years older than previous determinations from this unit (Loveridge *et al*., 1987).

KITTS DEPOSIT

In the area of the Kitts deposit (Figure 1), a sample of the Kitts metagabbro was collected from outcrop (Sample #GS-08-287) in an attempt to provide a maximum age constraint on the development of uranium mineralization. A minimum age constraint of 1881.8 ± 3.4 Ma for a quartz-feldspar porphyry dyke that crosscuts the deposit was previously reported by Sparkes *et al*. (2010). The metagabbro is interpreted to predate the deformation and uranium mineralization, and is assumed to be coeval with the Kitts Pillow Lava Formation (Marten, 1977; Evans, 1980). Late-stage, coarse-grained, pegmatitic zones within the metagabbro were targeted as having the highest probability for containing suitable minerals. These zones were largely composed of a white feldspar-rich groundmass hosting dark-green euhedral crystals of amphibole (Plate 6). In thin section, the metagabbro unit consists mostly of fine- to medium-grained actinolite−tremolite and lesser feldspar; locally rare fine-grained zircon crystals are observed within the feldspar-rich groundmass (Plate 7A, B). Processing of the sample yielded a small number of very strongly altered, turbid, euhedral zir-

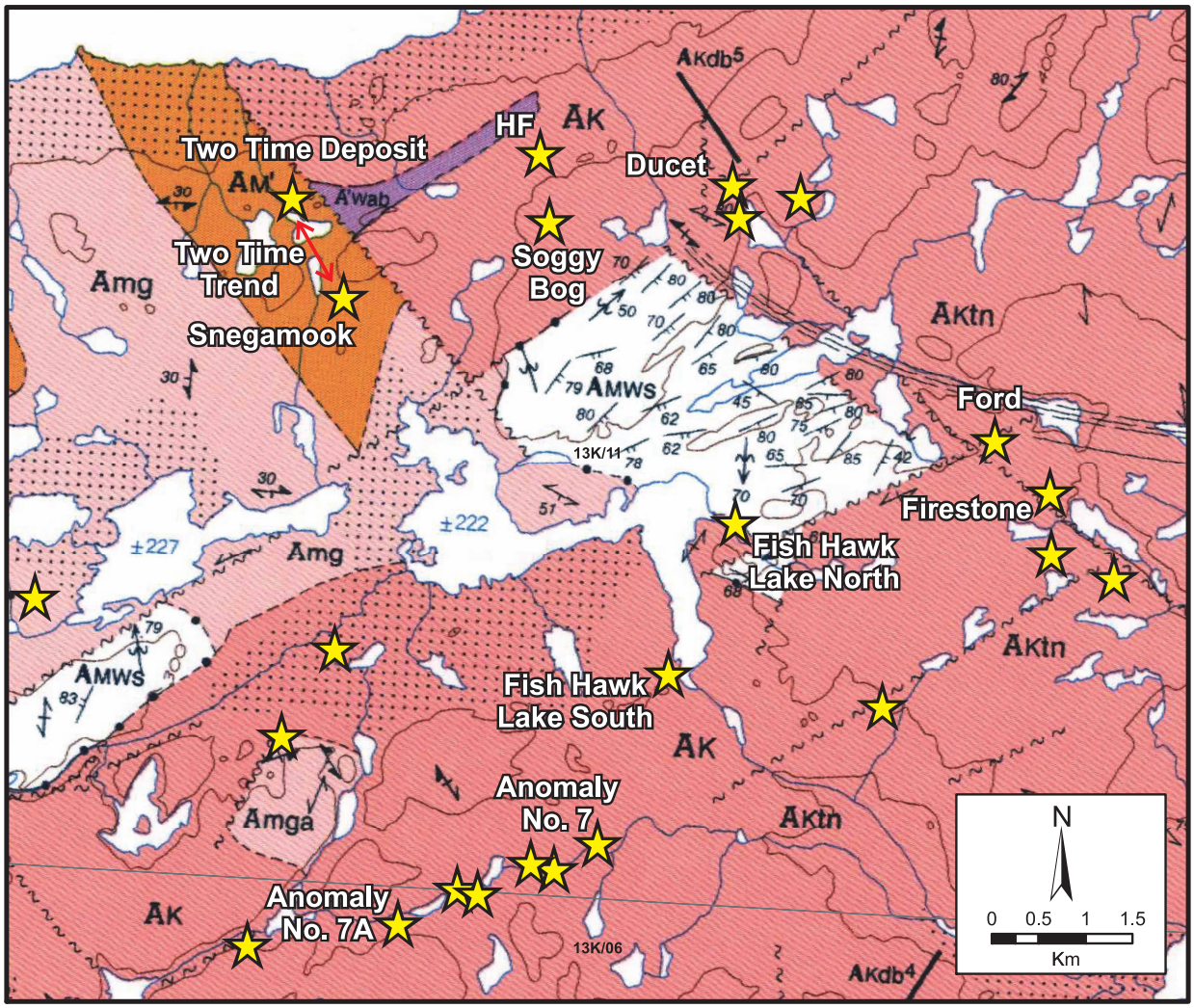

LEGEND

AMWs	Warren Creek Formation; grey to black mudstone, slate, siltstone, sandstone, minor limestone, dolostone and chert	AK	Tonalitic, granodiorite, and rare granite containing 10-15% biotite or hornblende, or both; medium- to coarse-grained, foliated to gneissic and locally schlieric
AKdb^5	Diabase 5 m wide	AKtn	Tonalitic rocks
Amg	Migmatite; felsic, gneissic, undivided metaplutonic rocks derived from middle Archean rocks.	Am'	Tonalitic gneiss; compositionally well preserved Maggo Gneiss
Amga	Mobilizate derived during intrusion of the Kanairiktok Intrusive Suite (AK); screen migmatic	A'wab	Amphibolite; commonly associated with ultramafics and rare laminae and layers of ferruginous or aluminous metasediments

★ Uranium occurrence

Figure 2. *Excerpt from the 1:100 000 geological map of Ermanovics (1992), outlining the distribution of the main geological units in the area of the Two Time deposit and Fish Hawk Lake prospects as well as the location of uranium occurrences as compiled from company websites and press releases.*

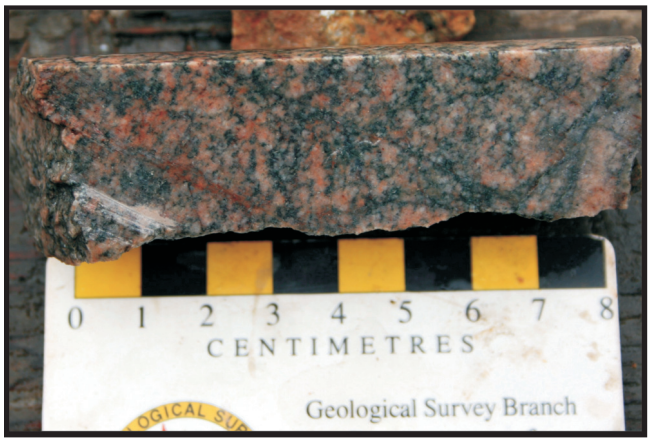

Plate 1. *Representative photograph of the fine- to medium-grained quartz monzodiorite–tonalite phase selected for geochronological study; Snegamook prospect (DDH SN-08-08, 50 m depth). Note the pale pink coloration of the sample is due to the development of weak hematite alteration and not the presence of potassium feldspar, as indicated by sodium cobaltinitrite staining.*

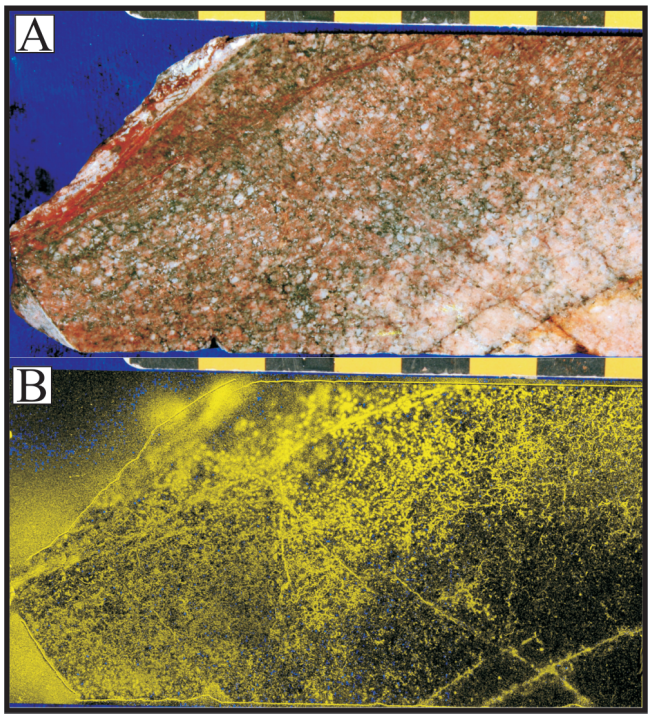

Plate 2. A) *Mineralized sample collected several metres above the area sampled for geochronological study; Snegamook prospect (DDH SN-08-08, 47.5 m depth); and* B) *Autoradiograph of (A) outlining the areas of radioactivity in yellow, minus the outline of the sample. Note the fracture-hosted and disseminated nature of the radioactivity that accompanies the pervasive hematite alteration.*

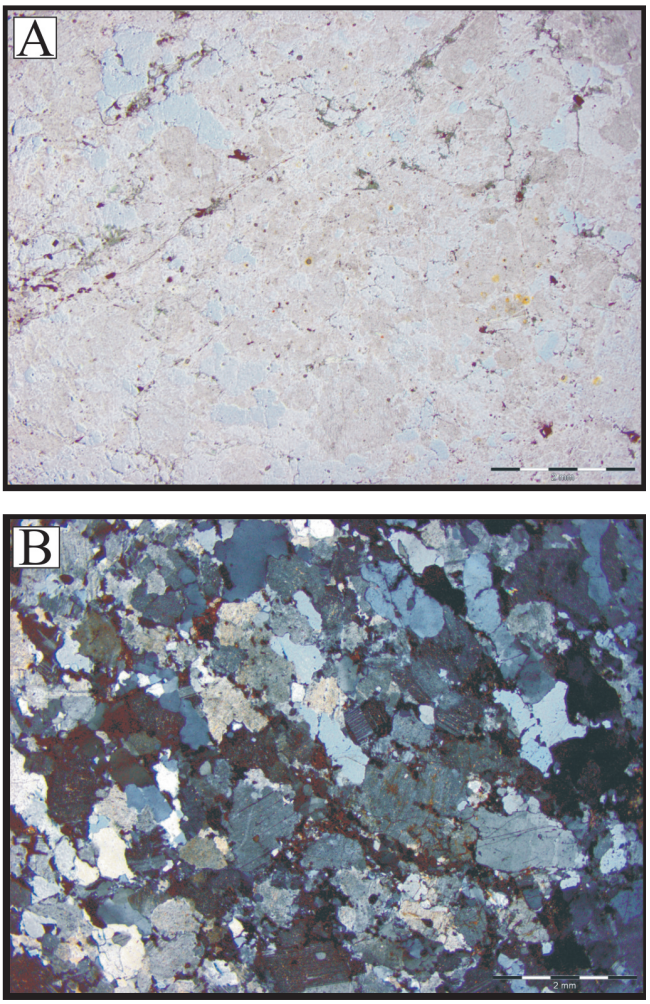

Plate 3. *Photomicrographs displaying the typical texture of the quartz monzodiorite–tonalite unit that was sampled as part of this study.* A) *Well-developed interlocking plagioclase and quartz groundmass hosting rare opaque oxide minerals that largely occur as fine-grained disseminations along grain boundaries (GS-09-44, PPL); and* B) *Cross-polarized view of (A).*

Plate 4. (opposite page) *Select mineral separates obtained from geochronological samples discussed in the text.* A) *Zircon from sample GS-09-44;* B) *Monazite from sample GS-09-44;* C) *Zircon from sample GS-08-215;* D) *Dark-coloured titanite from sample GS-08-215;* E) *Clear titanite from sample GS-08-215;* F) *Rutile from sample GS-08-215;* G) *Zircon from sample GS-08-229;* H) *Titanite from sample GS-08-229;* I) *Light-coloured titanite from sample GS-08-235; and* J) *Dark-coloured titanite from sample GS-08-235.*

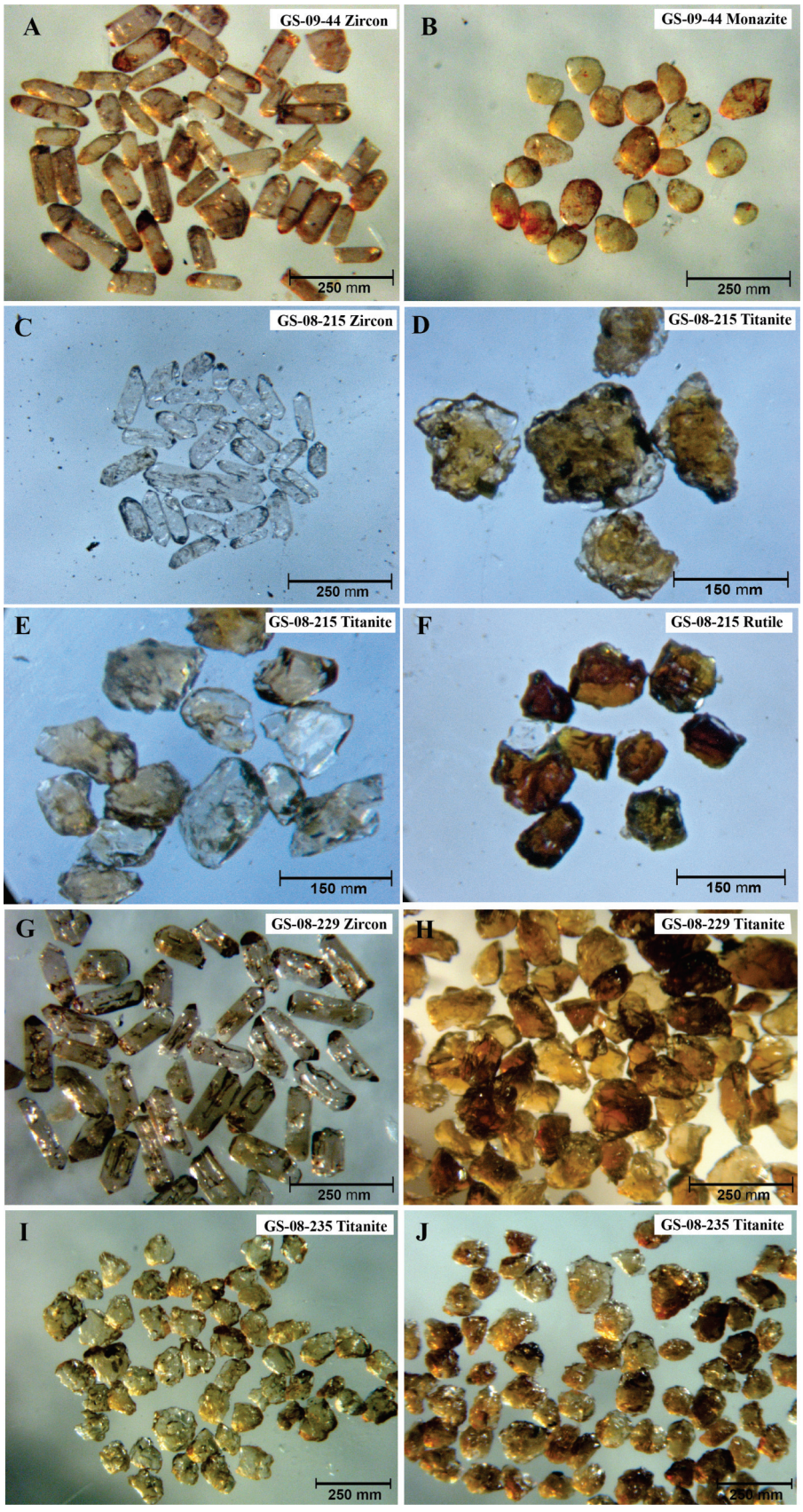

Plate 4. *Caption on opposite page.*

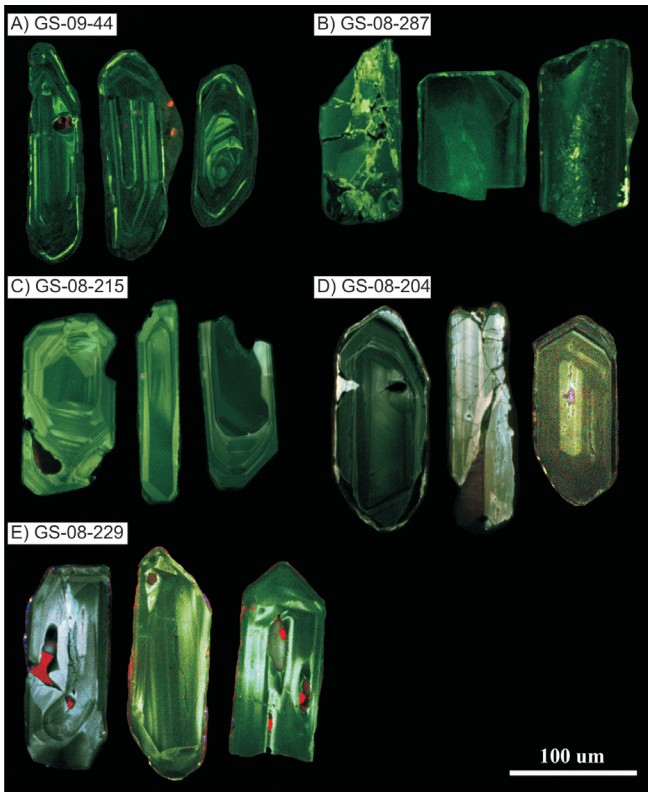

Plate 5. *Cathodoluminescence images for select grains outlining the typical textures observed within zircon separates obtained from the geochronological samples discussed in the text.* A) *Two Time deposit, GS-09-44;* B) *Kitts deposit, GS-08-287;* C) *Michelin deposit host rock, GS-08-215;* D) *Michelin deposit intrusion, GS-08-204; and* E) *Jacques Lake deposit intrusion, GS-08-229.*

con inferred to represent an igneous population (Plate 5). After the Mattinson (2005) chemical abrasion procedure (CA-TIMS), only a few tiny clear zircon remnants remained. Four analyses are concordant to 6% discordant and yield a line with an intercept age of 2018 +15/-8 Ma (Figure 3B). The concordant analysis alone gives a $^{207}Pb/^{206}Pb$ age of 2016 ± 9 Ma; the lower intercept is 744 +380/-290 Ma. The age of 2018 +15/-8 Ma is interpreted as the age of crystallization for the metagabbro unit and provides a maximum age constraint on the development of uranium mineralization. This age also agrees with the inference of Ketchum *et al.* (2001) based on detrital zircons from underlying metasedimentary rocks.

MICHELIN DEPOSIT

At the Michelin deposit (Figure 1), a sample of the metavolcanic rock hosting uranium mineralization was collected (Sample #GS-08-215; DDH M07-072, 439m depth) to compare its age with other ages from elsewhere in the Ailik Group (*cf.*, Hinchey and LaFlamme, 2009 and references therein), in addition to providing a maximum age limit on the development of uranium mineralization for the deposit. The sample was collected approximately 10 m below a mineralized intersection, which assayed 0.07% U_3O_8 over 3 m (Barrett *et al*., 2008). The host rock consists of a pale-grey, weakly feldspar-phyric metavolcanic unit (Plate 8), inferred to be part of an extensive sequence of deformed subaerial ash-flow tuff (*cf.,* Evans, 1980 and references therein). In thin section, this sample consists of a fine-grained matrix of quartz and feldspar hosting lesser phenocrysts of a similar composition (Plate 9A, B). The matrix is host to amphibole, biotite, opaque oxides (primarily consisting of magnetite) and titanite, with the later commonly forming rims around the oxide minerals, but also forming subhedral crystals locally intergrown with biotite (Plate 9C, D).

The geochronological sample yielded a large number of euhedral elongate prisms of high-quality zircon (Plate 4) with simple internal zonation as shown under cathodoluminescence (Plate 5). Three analyses, each containing three or four sharp prisms, yield tightly overlapping concordant data points that give a weighted average $^{207}Pb/^{206}Pb$ age of 1858 ± 2 Ma (MSWD=0.34; Figure 3C). Titanite in this rock shows a complicated age distribution (Figure 3D and E), with several generations of titanite growth indicated. Dark-brown grains with clear overgrowths (*cf.*, Plate 4D; T1, T2) and a grain with a 'raspberry' textured overgrowth (T3) define a line with a 75% probability of fit, using the calculation of Davis (1982), from 1609 ± 25 Ma to 1031± 21 Ma, anchored on concordia with 2 analyses of single small euhedral grains (Figure 3D). The uncertainty on the lower intercept age is quite large and an alternate approach, reporting the average $^{206}Pb/^{238}U$ age of the 2 concordant analyses (T4, T5) with their total 2 σ error limits, gives 1035 ± 10 Ma (Figure 3D). This linear pattern indicates growth of metamorphic titanite euhedra during a Labradorian event, followed by a second metamorphic event that crystallized additional titanite of Grenvillian age, as raspberry-textured overgrowths on the 1609 Ma titanite crystals, and as separate euhedral crystals. A second cluster of 3 concordant titanite single grain analyses (T6, T7, T8) overlap with $^{206}Pb/^{238}U$ ages of 1002, 1003 and 1006 Ma. The weighted average of these three analyses is 1003 ± 4 Ma (MSWD=0.40; Figure 3E). In addition, a third pair of concordant, clear euhedral titanite (T9, T10) have $^{206}Pb/^{238}U$ ages of 982 and 984 Ma, and these yield a weighted average age of 982 ± 3 Ma (MSWD=0.30; Figure 3E). These four separate titanite ages are interpreted to represent a complex metamorphic history, and illustrate the presence of Labradorian and Grenvillian deformation in the area of the Michelin deposit. In addition, clearly visible dark cores and clear overgrowths are present in the two generations of titanite that fit the line from 1609 to 1035 Ma; the corresponding $^{208}Pb/^{206}Pb$ ratios of the older 1609 Ma titanite are higher than those of the younger 1035 Ma titanite. These

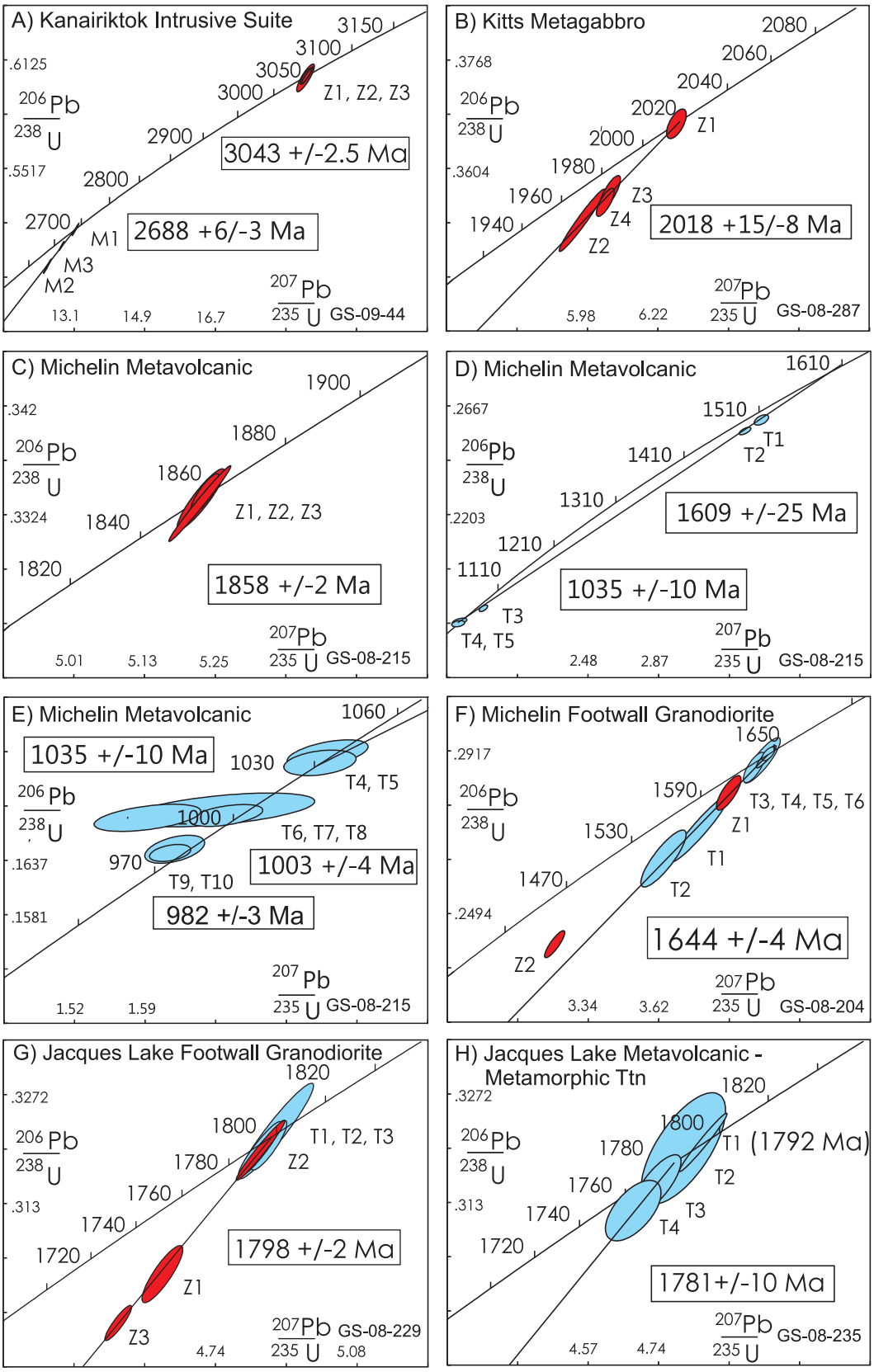

Figure 3. *Concordia diagrams of U–Pb results from zircon, monazite and titanite analyses for samples discussed in the text. Error ellipses are at the 2σ level. Refer to Table 1 for sample location and description.*

Table 1. U–Pb Zircon, titanite and monazite data for samples from the CMB of Labrador; UTM's for each sample are provided in NAD 27, Zone 21 coordinates

Fraction	Weight [mg]	Concentration U [ppm]	Concentration Pb rad [ppm]	Measured total common Pb [pg]	Measured $^{206}Pb/^{204}Pb$	Corrected Atomic Ratios (c) $^{208}Pb/^{206}Pb$	$^{206}Pb/^{238}U$		$^{207}Pb/^{235}U$		$^{207}Pb/^{206}Pb$		Age [Ma] $^{206}Pb/^{238}U$	$^{207}Pb/^{235}U$	$^{207}Pb/^{206}Pb$
GS-09-44 Two Time Quartz Monzodiorite (230994,6052981)															
Z1 2 sml prm E	0.002	59	44.8	4.5	1001	0.2273	0.60240	632	18.9997	1840	0.22875	124	3039	3042	3043
Z2 2 sml prm E	0.002	33	25.9	4.1	637	0.2649	0.60331	362	19.0072	1160	0.22849	74	3043	3042	3042
Z3 3 sml prm E	0.003	81	59.6	4.1	2248	0.1786	0.60369	398	19.0396	1242	0.22874	44	3045	3044	3043
M1 2 lrg pale yel A	0.003	2711	5995.6	13	19559	3.7518	0.51760	270	13.1348	690	0.18404	14	2689	2689	2690
M2 1 lrg pale yel A	0.002	1906	4392.4	14	6404	4.1746	0.49699	324	12.4168	810	0.18120	18	2601	2636	2664
M3 1 lrg pale yel A	0.002	2306	5885.6	25	4477	4.6153	0.50844	210	12.7831	540	0.18235	12	2650	2664	2674
GS-08-287 Kitts Metagabbro (340475, 6097407)															
Z1 3 prm E	0.002	92	39.1	2.1	1519	0.2253	0.36715	182	6.2829	274	0.12411	50	2016	2016	2016
Z2 2 clr euh E	0.002	333	144.4	3.6	4067	0.3051	0.35257	386	5.9615	634	0.12263	32	1947	1970	1995
Z3 1 euh prm E	0.001	853	383.0	3.5	5424	0.3376	0.35677	210	6.0566	290	0.12312	44	1967	1984	2002
Z4 1 poor euh prm E	0.001	180	77.1	4.4	935	0.2779	0.35529	174	6.0406	248	0.12331	38	1960	1982	2005
GS-08-215 Michelin Host Volcanic Rock (307146, 6051898)															
Z1 3 clr sharp euh E	0.004	287	102.8	2.5	11060	0.1308	0.33426	144	5.2326	198	0.11354	26	1859	1858	1857
Z2 4 clr sharp euh E	0.006	96	34.0	2.2	5466	0.1271	0.33378	218	5.2259	328	0.11355	32	1857	1857	1857
Z3 3 clr sharp euh E	0.004	163	57.9	1.6	9673	0.1257	0.33338	274	5.2241	430	0.11365	16	1855	1857	1859
T1 1 best clr dk A	0.002	167	46.7	13	335	0.1510	0.26066	180	3.4371	326	0.09564	80	1493	1513	1541
T2 1 clr euh crystal	0.002	162	46.4	27	213	0.2040	0.25593	130	3.3467	266	0.09484	56	1469	1492	1525
T3 1 rasp overgrowth	0.002	270	47.4	22	221	0.0550	0.18032	114	1.9025	192	0.07652	60	1069	1082	1109
T4 1 clr euh pale brn	0.002	91	14.9	12	178	0.0170	0.17469	116	1.7709	328	0.07353	118	1038	1035	1028
T5 1 sml clr A	0.002	63	10.5	34	57	0.0437	0.17374	108	1.7633	294	0.07361	116	1033	1032	1031
T6 1 sml clr A	0.001	121	19.0	33	57	0.0121	0.16889	142	1.6654	760	0.07152	300	1006	995	972
T7 1 clr pale brn	0.002	137	21.5	18	175	0.0134	0.16832	92	1.6704	296	0.07198	114	1003	997	985
T8 1 clr dk brn A	0.002	193	30.1	45	85	0.0117	0.16808	114	1.5923	432	0.06871	168	1002	967	890
T9 2 best clr dk A	0.002	231	35.2	14	271	0.0009	0.16484	118	1.6193	242	0.07125	94	984	978	965
T10 1 grain	0.002	157	23.8	12	278	0.0001	0.16446	72	1.6148	166	0.07121	68	982	976	964
T11 1 rasp overgrowth	0.002	1186	70.1	32	223	0.0985	0.05852	86	0.6128	98	0.07595	76	367	485	1094
GS-08-204 Michelin Footwall Granodiorite (306492, 6051177)															
Z1 1 lrg prm A	0.003	574	163.6	2.0	15415	0.0795	0.28079	366	3.8979	398	0.10068	82	1595	1613	1637
Z2 1 lrg prm A	0.003	907	232.8	2.4	16910	0.1394	0.24147	286	3.2066	326	0.09631	58	1394	1459	1554
T1 1 lrg dk brn A	0.005	1087	500.7	71	1316	0.8648	0.27146	706	3.7821	944	0.10105	82	1548	1589	1643
T2 1 clr dk brn A	0.005	969	422.2	70	1165	0.8139	0.26372	604	3.6387	736	0.10007	122	1509	1558	1625
T3 1 clr dk brn A	0.005	823	444.6	50	1515	1.0612	0.28923	482	4.0303	592	0.10106	84	1638	1640	1644
T4 1 dk brn clr A	0.002	1141	596.3	29	1449	0.9808	0.29091	146	4.0553	210	0.10110	42	1646	1645	1644

T5 1 clr dk brn A	0.002	822	410.8	19	1601	0.8944	0.29018	236	4.0467	320	0.10114	34	1642	1644	1645
T6 1 equant dk brn A	0.002	1361	522.6	20	2431	0.4489	0.28738	322	3.9988	348	0.10092	74	1628	1634	1641
GS-08-229 Jacques Lake Footwall Granodiorite (332769, 6065965)															
Z1 4 3:1 prm melt icl	0.006	253	82.0	2.1	13757	0.1280	0.30380	304	4.6125	402	0.11012	56	1710	1752	1801
Z2 2 3:1 prm	0.003	224	73.3	2.3	5867	0.0743	0.32060	264	4.8681	352	0.11013	44	1793	1797	1802
Z3 4 sml 3:1 prm	0.006	247	79.8	6.4	4310	0.1536	0.29743	188	4.5064	262	0.10989	30	1679	1732	1798
T1 2 lrg dk brn clr	0.006	555	205.5	47	1447	0.2242	0.32245	508	4.8854	736	0.10988	56	1802	1800	1797
T2 3 lrg dk brn clr	0.009	480	175.4	55	1587	0.2174	0.31992	320	4.8480	478	0.10991	24	1789	1793	1798
T3 6 lrg dk brn clr	0.018	274	115.9	55	1814	0.4258	0.32007	294	4.8464	422	0.10982	38	1790	1793	1796
GS-08-235 Jacques Lake Host Volcanic Rock (332815, 6065831)															
T1 4 med clr dk brn	0.008	353	123.0	85	688	0.1512	0.32086	312	4.8477	468	0.10958	22	1794	1793	1792
T2 3 med clr dk brn	0.006	299	104.5	121	313	0.1588	0.32008	594	4.7999	830	0.10876	156	1790	1785	1779
T3 3 med clr lt brn	0.006	46	15.5	23	255	0.1337	0.31540	314	4.7357	476	0.10890	74	1767	1774	1781
T4 4 med lt brn	0.008	75	26.6	51	247	0.2180	0.31193	324	4.6788	548	0.10879	110	1750	1763	1779

Notes: Z=zircon, M=monazite, T=titanite, 1,2=number of grains, lrg=large, clr=clear, sml=small, med=medium, yel=yellow, brn=brown, lt=light, dk=dark, rasp=raspberry, icl=inclusion, prm =prism, euh=euhedral, A=abraded (cf. Krogh, 1982). E=etched (cf. Mattinson, 2005). Weights were estimated.
* Atomic ratios corrected for fractionation, spike, laboratory blank of 1-4 picograms of common lead, and initial common lead at the age of the sample calculated from the model of Stacey and Kramers (1975), and 0.5-1 picogram U blank. Two sigma uncertainties are reported after the ratios and refer to the final digits.

Plate 6. *Photograph of the coarse-grained pegmatitic zone locally developed within the Kitts metagabbro, which was sampled for U–Pb geochronology.*

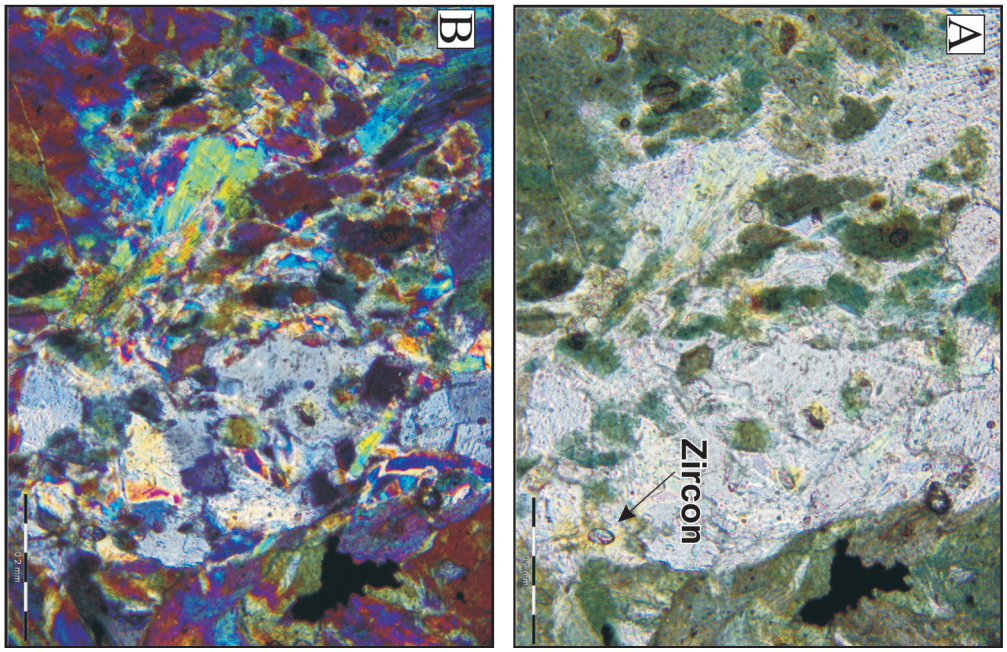

Plate 7. A) *Photomicrograph of the actinolite–plagioclase-rich groundmass of the pegmatitic material; note the occurrence of a fine-grained zircon crystal in the lower right hand corner; and* B) *Cross-polarized view of (A).*

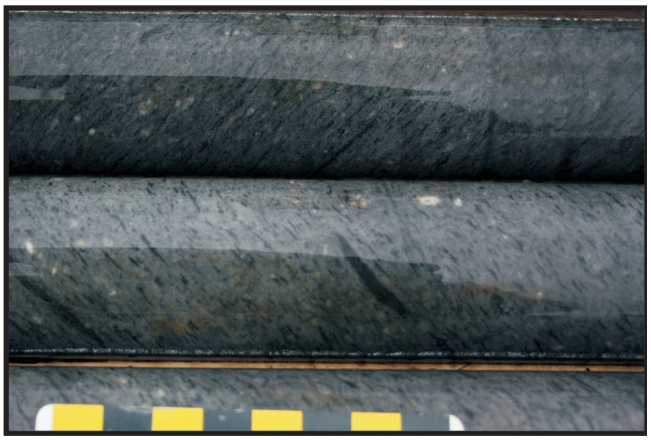

Plate 8. *Representative photograph of the metavolcanic host rock at the Michelin deposit; note the unit displays a prominent foliation, which is largely highlighted by the development of biotite and amphibole within the sample.*

data give calculated minimum Th/U ratios of 0.75 to 1.02 for the older brown titanite (T1, T2); in contrast the younger clear euhedral titanite grains (T9, T10) have essentially no ^{208}Pb and have $^{208}Pb/^{206}Pb$ ratios of 0.0009 and 0.0001, respectively. These indicate extremely low Th/U ratios of 0.003 and <0.001 for the 982 Ma titanite generation, but with normal U concentrations. Rutile is also present in this sample as separate, high quality grains (Plate 4F). Analysis of two fractions showed that they contain no uranium, so no age was obtained.

In the vicinity of the Michelin deposit, the metavolcanic rocks of the Aillik Group are intruded by a number of different plutonic phases that range from granite to diorite in composition. An undeformed dyke that ranged in composition from granodiorite to diorite was selected for geochronological study from an area of deep drilling, with the sample being collected from an intrusion at a vertical depth of approximately 1100 m below surface (Sample #GS-08-204; DDH M07-075A, 1128 m depth). The sample, which exhibits sharp intrusive contacts with the surrounding foliated metavolcanic country rock (Plate 10), has a medium-grained groundmass primarily composed of feldspar and lesser quartz, along with biotite and hornblende (Plate 11A). The intrusion also contains a large amount of apatite, which locally becomes concentrated in late-stage 'pockets' of interstitial feldspar along with lesser epidote (Plate 11B). The sample produced a population of both titanite and zircon. Six analyses of single large grains of dark-brown titanite and two zircon analyses have been carried out. The two zircon analyses give discordant data but Z1 fits on the line with the 6 titanite analyses. This line (77% probability of fit), anchored by 4 concordant titanite, gives an age for igneous crystallization of 1644 ± 4 Ma (Figure 3F); the lower intercept is 31 ± 46 Ma. It is interpreted that all titanite is of igneous origin in this sample. In addition, the age provides a minimum age on the development of the foliation within the adjacent country rock, which is truncated by the intrusion.

JACQUES LAKE DEPOSIT

In the area of the Jacques Lake deposit (Figure 1) an undeformed intermediate intrusive unit forms the footwall to the main zone of uranium mineralization. The intrusion ranges from granodiorite to quartz monzonite in composition and displays a sharp intrusive contact with the adjacent intermediate metavolcanic rocks, truncating the foliation developed within the country rock (Plate 12). The intrusion consists of a medium-grained feldspar-rich groundmass, containing quartz and lesser biotite and hornblende in addition to fine-grained disseminated opaque minerals (Plate 13A). In thin section, this unit contains clots of mafic minerals, oxides, titanite, and zircon, and in some cases, well-developed reaction rims of titanite around the oxide minerals (Plate 13B). In the rock texture, there are also many euhedral sphenoid-morphology grains of titanite as well. A sample of this unit was collected from drillcore (Sample #GS-08-229; DDH JL07-058A, 236 m depth) and yielded coarse-grained zircon and titanite. The zircons are coarse-grained euhedral prisms and many contain inclusions, including quite large melt inclusions. Three zircon analyses of 2 or 4 grains are concordant or a few percent discordant, and a zircon-only age calculation gives 1799 ± 4 Ma (weighted average of $^{207}Pb/^{206}Pb$ ages; 95% CI, MSWD= 0.53; Figure 3G). Three titanite analyses are all concordant on top of the concordant zircon analysis and an age calculated as the weighted average of $^{207}Pb/^{206}Pb$ ages of all 6 analyses is 1798 ± 2 Ma (MSWD=0.35). This age is interpreted to be the crystallization age of the unit and also provides a minimum age limit for the foliation developed within the adjacent country rock as well as the uranium mineralization contained within.

At the Jacques Lake deposit, a sample of the intermediate metavolcanic host rock to mineralization was also collected from drillcore (Sample #GS-08-235; DDH JL07-060, 169 m depth). The sample failed to produce a significant population of zircon, but did yield a large population of coarse-grained titanite. In thin section, the sample consists of a fine-grained matrix of quartz and feldspar along with coarser grained hornblende, biotite, titanite and abundant opaque oxide minerals, primarily in the form of magnetite (Plate 14A, B). The titanite is dispersed throughout the rock and many grains are anhedral or rounded and can locally be seen rimming the oxide phase. The sample contained both dark- and light-coloured titanite that may represent two different generations, with fairly certain core-overgrowth relationships in some grains with darker cores and lighter rims

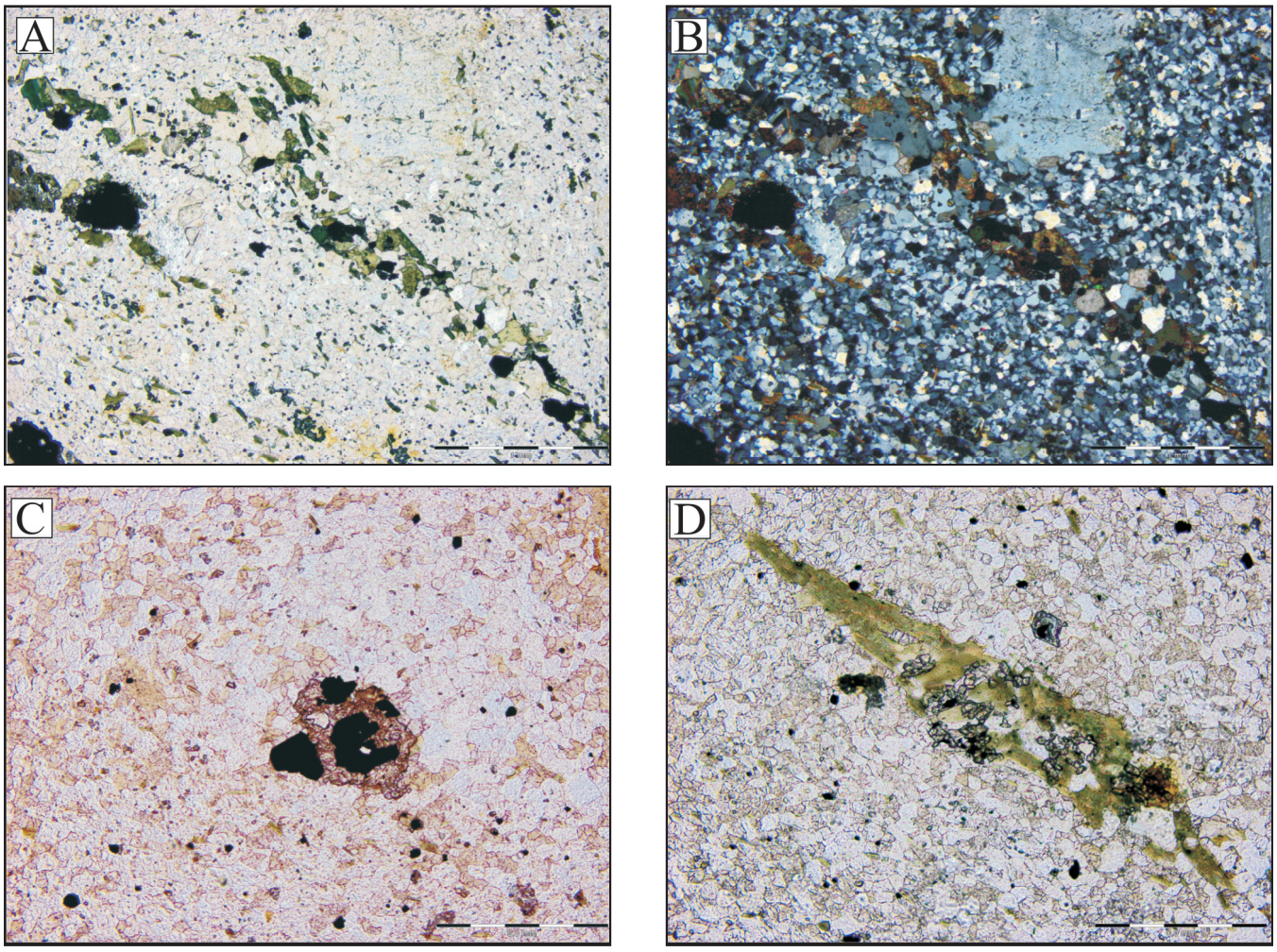

Plate 9. *Photomicrographs displaying the typical textures and mineral relationships developed within the metavolcanic host rock of the Michelin deposit.* A) *Fine-grained matrix of quartz and feldspar along with abundant opaque oxides, largely magnetite, and lesser dark-green biotite and amphibole;* B) *Cross-polarized view of (A);* C) *Opaque oxides rimmed by one of the multiple generations of titanite; and* D) *Dark-green biotite intergrown with titanite.*

(Plate 4); further detailed SEM imagery is required to confirm these relationships. Two analyses of both the dark and light grains were carried out. The one high-quality analysis of a dark titanite fraction is concordant at 1792 Ma (T1). Two analyses of light titanite have dramatically lower U contents, and $^{207}Pb/^{206}Pb$ ages of 1781 and 1779 Ma (T3, T4; Figure 3H). Whereas these have a higher proportion of common lead, the ages are still quite robust and are clearly younger than those of the dark-brown titanite. A weighted average $^{207}Pb/^{206}Pb$ age of the two analyses of the younger light-brown titanite gives 1781 ± 10 Ma (MSWD=0.03, 95% CI). The tentative interpretation is that these are two generations of metamorphic titanite contained within the sample, one at *ca.* 1792 Ma, and another at *ca.* 1781 Ma; these ages are slightly younger than the post-mineralization intrusions in the area (*cf.*, Sparkes and Dunning, 2009) and therefore provide evidence for post-mineralization metamorphic events.

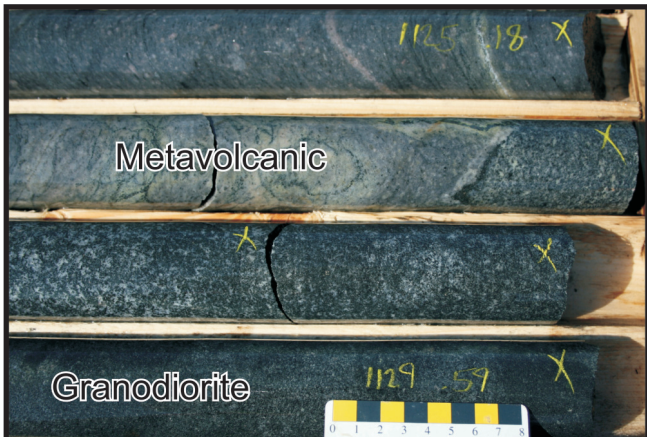

Plate 10. *Photograph displaying the sharp intrusive contact between the foliated metavolcanic country rock and the relatively undeformed fine- to medium-grained granodiorite intrusion at the Michelin deposit (DDH M07-75A; 1130 m depth).*

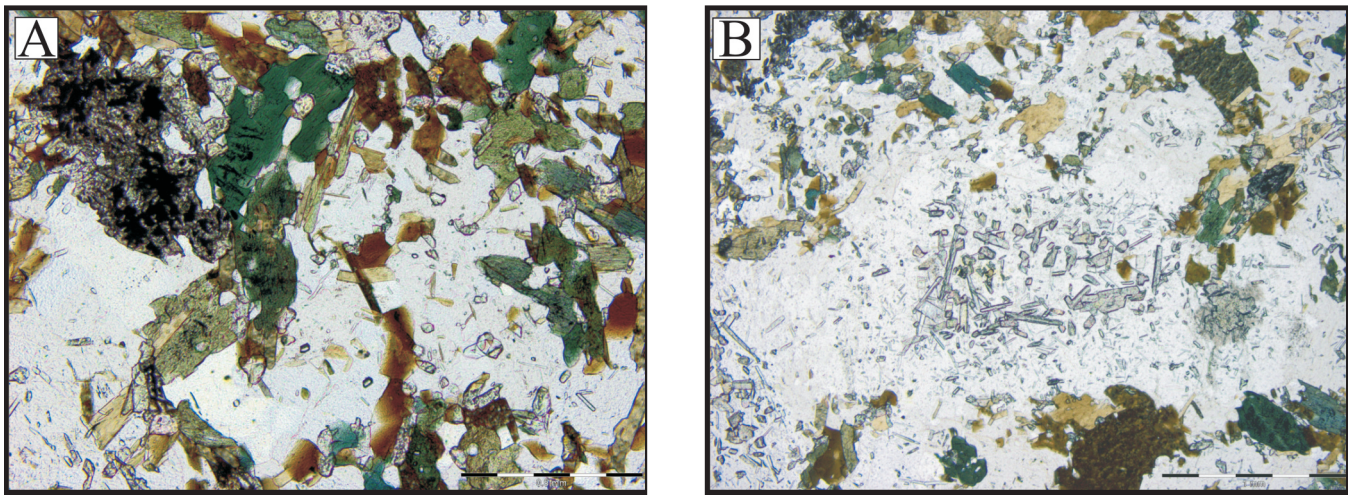

Plate 11. *Photomicrographs of the granodiorite intrusion shown in Plate 10.* A) *Medium-grained groundmass consisting of feldspar and lesser quartz, along with biotite and hornblende along with lesser opaque oxide minerals rimmed by titanite; and* B) *Late-stage, plagioclase-rich 'pockets' hosting abundant apatite along with lesser epidote.*

Plate 12. *Photograph highlighting the sharp intrusive contact between the foliated metavolcanic country rock and undeformed medium-grained granodiorite to quartz monzonite at the Jacques Lake deposit (DDH JL07-58A; 230 m depth).*

SUMMARY AND DISCUSSION

Figure 4 provides a summary of the ages reported herein along with other relevant ages from previous work that have been discussed in the text. Uranium mineralization hosted within the Archean basement rocks in the area of the Two Time deposit was first discovered in the mid-2000s and represents a relatively recent discovery within the CMB. New data presented herein demonstrates the Archean age of the plutonic host rock to the uranium mineralization; however, the geological interpretation of the area indicates that the uranium mineralization is potentially much younger. At the Two Time deposit, the *ca.* 3000 Ma host rock to the uranium mineralization is crosscut by an extensive northwest–southeast-trending fault system hosting zones of cataclastic breccia, within which the uranium mineralization is developed. This mineralized structure is developed roughly subparallel to a northwest–southeast-trending fault structure that affects rocks of the Moran Lake Group as shown on regional geology maps for the area (Figure 2). As a result, these structures along with the contained mineralization are inferred to be younger than the overlying *ca.* 2100 Ma siliciclastic sedimentary rocks of the Moran Lake Group. A $^{207}Pb/^{206}Pb$ age of 1774 ± 9 Ma is reported for uranium mineralization developed at the Anomaly No. 7 prospect (Wilton and Longerich, 1993; Figure 2); however, similar $^{207}Pb/^{206}Pb$ ages from elsewhere within the CMB have locally been shown to be significantly younger than the actual age of mineralization and cannot be relied upon (*e.g.*, Sparkes *et al*., 2010).

Mineralization developed along the Two Time Trend is locally crosscut by mafic dykes that will be the focus of future geochronological studies in the area. Currently, the only existing age control on the formation of the uranium mineralization at the Two Time deposit is the 3043 ± 2.5 Ma age provided for the quartz monzodiorite−tonalite host rock. This age is some 180 Ma older than the reported age of 2858 +4/-3 Ma by Loveridge *et al*. (1987), which is also reported to be from rocks of the Kanairiktok intrusive suite. Such evidence suggests that rocks currently grouped within the Kanairiktok intrusive suite represent several discrete intrusions with considerable variation in age.

The Post Hill Group, which is inferred to be coeval with rocks of the Moran Lake Group (*cf.*, Marten, 1977; Wardle and Bailey, 1981), hosts some of the oldest mineralization within the CMB. The previously reported age of 1881.8 ±

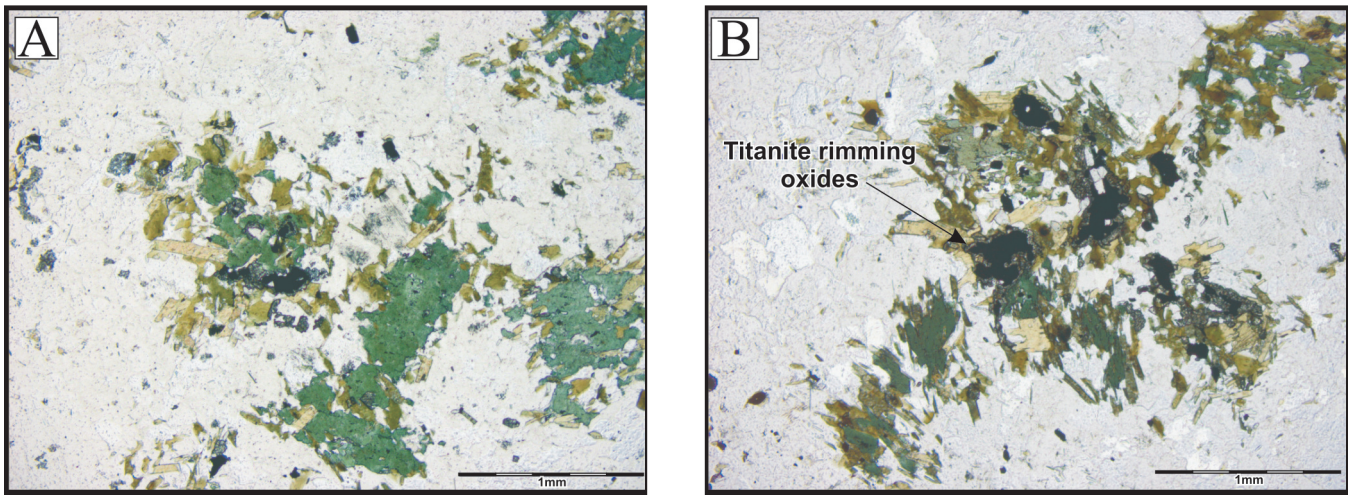

Plate 13. *Photomicrograph of the intrusion shown in Plate 12.* A) *Medium-grained intrusion containing light-green amphibole being replaced by an assemblage consisting of dark-green to brown biotite, opaque oxide minerals and titanite, all of which is supported within a plagioclase-rich groundmass along with lesser quartz; and* B) *Similar relationship to that shown in (A), illustrating the alteration of hornblende to an assemblage consisting of biotite, opaque oxide minerals and titanite.*

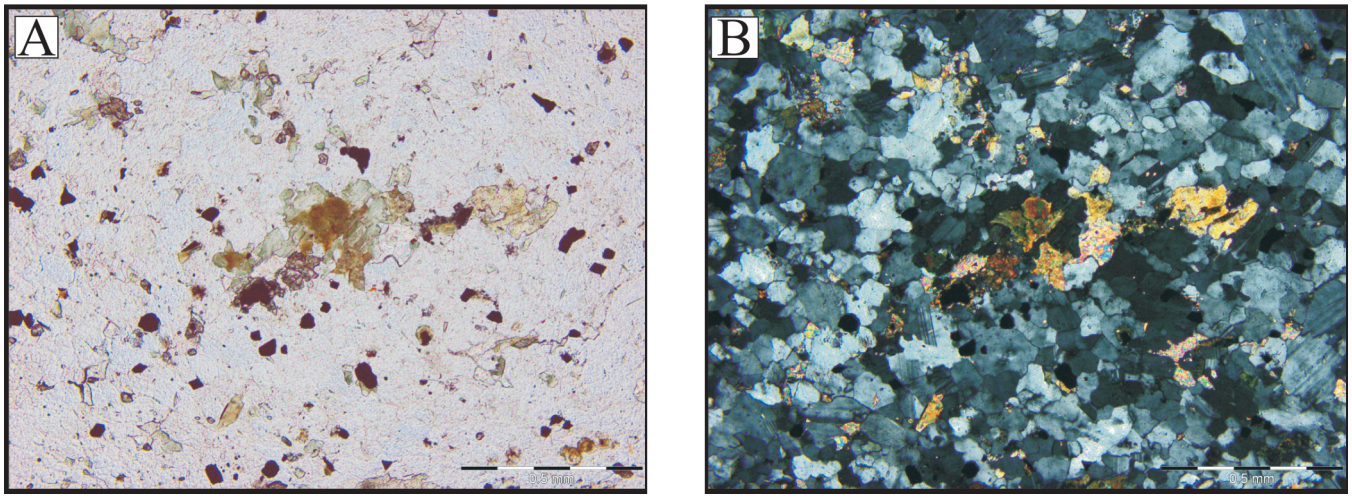

Plate 14. *Photomicrographs displaying the typical texture of the intermediate metavolcanic host rock at the Jacques Lake deposit.* A) *Fine-grained matrix of quartz and feldspar hosting hornblende, biotite, titanite and opaque oxide minerals; and* B) *Cross-polarized view of (A).*

3.4 Ma (Sparkes *et al*., 2010) for a quartz-feldspar porphyry dyke crosscutting mineralization at the Kitts deposit demonstrates that the mineralization is older than that at the Michelin deposit. The age of 2018 +15/-8 Ma from the Kitts Metagabbro provides a maximum limit on mineralization in the area, which can now be bracketed between 2030 and 1880 Ma, on the basis of existing geochronological data (Figure 4). The high-grade Kitts deposit has been the main focus of study within this area; however, other deposits that occur along strike, including Gear, Inda and Nash are inferred to be of a similar age. This new geochronological data for the Post Hill Group is also in agreement with the existing data and stratigraphy as outlined by Ketchum *et al*. (2001) and provides the first evidence of an intrusive event of this age within the CMB.

The age of 1858 ± 2 Ma for the host metavolcanic sequence at the Michelin deposit is similar to that reported from the nearby Michelin Ridge, which produced an age of 1856 ± 2 Ma (Schärer *et al*., 1988). In the area of the Michelin deposit, a thick sequence of what is inferred to be a subaerial ash-flow tuff is host to intense albitic alteration along with associated hematization and uranium mineralization. The age for the host rock at the Michelin deposit provides a maximum age limit on the development of uranium mineralization in the area, and demonstrates that the alteration and

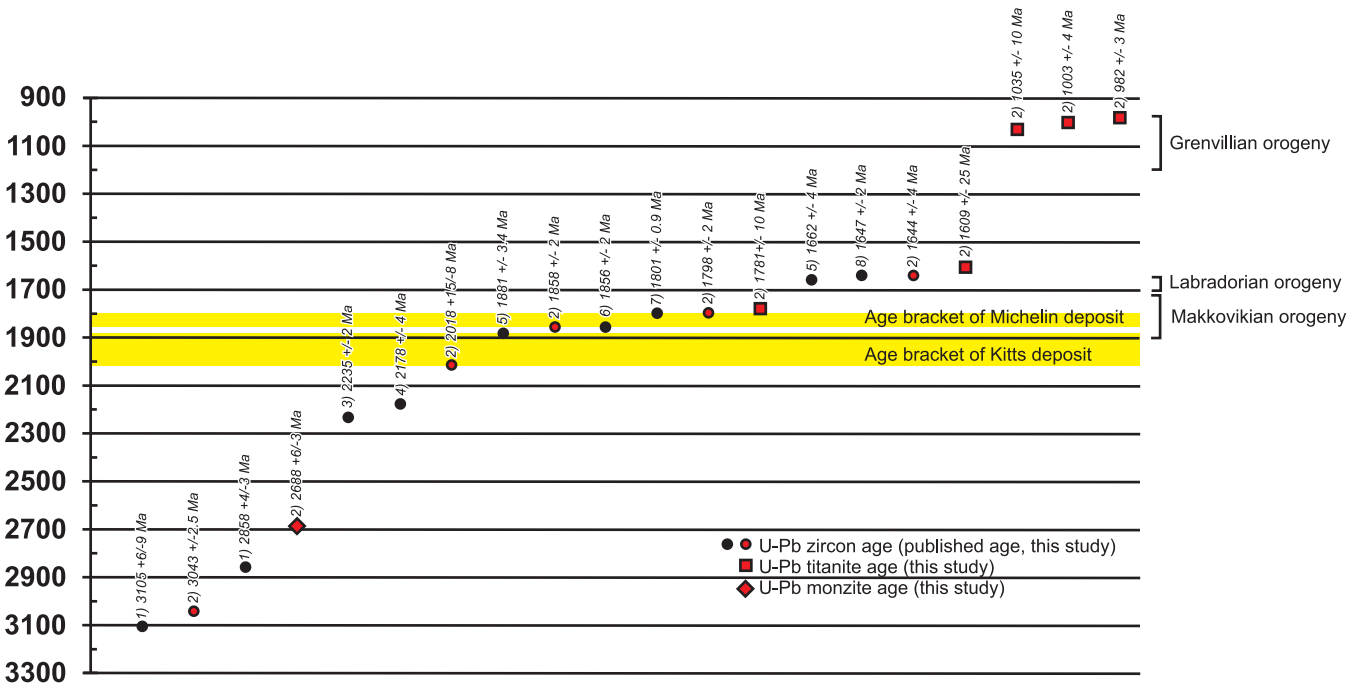

Figure 4. *Summary diagram outlining the geochronological data discussed in the text as well as relevant ages from other sources; 1) Loveridge* et al. *(1987); 2)* this study*; 3) Cadman* et al. *(1993); 4) Ketchum* et al. *(2001); 5) Sparkes* et al. *(2010); 6) Schärer* et al.*, 1988; 7) Sparkes and Dunning (2009); 8) Kerr* et al.*, 1992.*

associated mineralization is a distinct metallogenic event, one that forms at least 20 Ma after the formation of the Kitts deposit. If the mineralization developed at both the Michelin and Jacques Lake deposits are part of the same mineralizing event, then the minimum age for the Jacques Lake deposit could also be applied to the Michelin deposit, bracketing the mineralization between 1860 and 1800 Ma (Figure 4). This age bracket closely overlaps that of the regional D_3 shearing event outlined by Culshaw *et al.* (2000), which potentially represents the main uranium mineralizing event within the metavolcanic rocks of the Aillik Group. The age of 1644 ± 4 Ma for the intermediate intrusion at the Michelin deposit is similar to the reported age of 1647 ± 2 Ma from a sample of the Otter Lake-Walker Lake granite, collected some 9 km to the west of the Michelin deposit (Kerr *et al*., 1992). The Otter Lake-Walker Lake granite is part of the regionally extensive Labradorian plutonic assemblage and given the similar age of the intermediate intrusion at the Michelin deposit, it too is also likely linked to this event.

The presence of several generations of titanite within the host metavolcanic rock at the Michelin deposit provides evidence for multiple metamorphic events that overprint both the metavolcanic succession and the uranium mineralization contained within. The oldest titanite identified within the sample at 1609 ± 25 Ma comes close in age to the undeformed granodiorite intrusion (1644 ± 4 Ma), which postdates the main penetrative fabric within the metavolcanic host rock, and is likely linked to the Labradorian orogeny (Figure 4). Although the host metavolcanic rock contains a strong penetrative fabric that predates the *ca.*1650 Ma intrusion, no evidence of this older deformation is observed within the data. The younger titanite ages within the sample reveal distinct episodes of Grenvillian 'thermal' events, which may be linked with further deformation in the area. Given the evidence of older deformational events and the likely structural control on the formation of the inferred *ca.* 1860–1800 Ma Michelin deposit, these younger Grenvillian ages potentially represent the reactivation of an already existing structure during Grenvillian orogenesis. The youngest ages of *ca.* 1000 and 980 Ma are linked to extensional collapse of the Grenvillian orogeny (Rivers *et al*., 2002).

In the area of the Jacques Lake deposit, the host rock failed to produce a significant population of what could be interpreted as primary zircon but did contain abundant titanite that produced an age of 1781 ± 10 Ma. This titanite age provides evidence for a metamorphic event that is some 140 Ma older than that identified at the Michelin deposit. The Jacques Lake deposit is located farther north than the Michelin deposit and is thus farther from the Grenville front and likely was not affected by the same degree of deformation during Grenvillian events. The period of older deformation defined by the titanite broadly falls within the *ca*. 1900–1790 Ma age bracket for the Makkovikian orogeny

and is likely linked to this event. As the uranium mineralization at the Jacques Lake deposit has a defined minimum age of 1801 ± 0.9 Ma (Sparkes and Dunning, 2009), this *ca.* 1780 Ma deformation represents a post-mineralization metamorphic event. The age of 1798 ± 2 Ma for the intermediate intrusion within the footwall of the Jacques Lake deposit is similar in age to other *ca.* 1800 Ma intrusions in the region that have been attributed to syn- and posttectonic magmatism related to the Makkovikian orogeny (Kerr *et al*., 1992). At the Jacques Lake deposit, this relatively undeformed intrusion truncates an existing structural fabric within the metavolcanic country rock. Similar to observations made at the Michelin deposit, this older period of deformation is likely related to the regional D_3 shearing event outlined by Culshaw *et al.* (2000), and is potentially linked with the main uranium mineralizing event.

Ongoing efforts within the region will continue to further refine the constraints on the development of the various uranium mineralizing events. To date, existing geochronological data can be used to outline three main periods of uranium mineralization, which are: 1) 2030–1880 Ma, 2) 1860–1800 Ma, and 3) post 1650 Ma. Early interpretations for the genesis of uranium mineralization developed within the Post Hill Group, which falls within the 2030-1880 Ma time bracket, included both syngenetic (*e.g.*, Gandhi, 1978) and epigenetic (*e.g.*, Marten, 1977; Gower *et al*., 1982) models. The early epigenetic model inferred Michelin and Kitts to form from the same mineralizing event. Sparkes and Kerr (2008) classify both the Michelin and Kitts deposits as being the result of 'metamorphic–metasomatic' processes linked with regional deformation; however, geochronological data now indicate that the two are not part of the same mineralizing event. With regards to the contained uranium mineralization within the CMB, those deposits formed within the 1860–1800 Ma time period contain the most significant resource, and therefore represent the most economically significant metallogenic event within the region. The post-1650 Ma mineralization represents uranium mineralization contained within the felsic volcanic rocks of the Bruce River Group. This mineralization represents a small portion of uranium mineralization contained within the CMB; however, it demonstrates the prolonged period of uranium enrichment, which spans some 380 Ma based on existing data.

ACKNOWLEDGMENTS

We would like to thank Dylan Abbott for his assistance and perseverance in the field, and Sherri Strong and Amanda Langille for excellent work in the U–Pb geochronology and Scanning Electron Microscope laboratories.

REFERENCES

Bailey, D.G.
1979: Geology of the Walker-MacLean Lake area, 13K/9, 13J/12, Central Mineral Belt, Labrador. Newfoundland Department of Mines and Energy, Mineral Development Division, Report 78-3, 17 pages.

Barrett, S., Barbour, D. and Glover, J.
2008: Fifth year assessment report on diamond drilling exploration for licence 9412M on claims in the Ranjan Lake area, central Labrador. Newfoundland and Labrador Geological Survey, Assessment File LAB/1532, 2008, 555 pages.

Beavan, A.P.
1958: The Labrador uranium area. Proceeding of the Geological Association of Canada, Volume 10, pages 137-145.

Cadman, A.C., Heaman, L, Tarney, J., Wardle, R. and Krogh, T.E.
1993: U–Pb geochronology and geochemical variation within two Proterozoic mafic dyke swarms, Labrador. Canadian Journal of Earth Sciences, Volume 30, No. 7, pages 1490-1504.

Culshaw, N., Ketchum, J. and Barr, S.
2000: Structural evolution of the Makkovik Province, Labrador, Canada: Tectonic processes during 200 Myr at a Paleoproterozoic active margin. Tectonics, Volume 19, No. 5, pages 961-977.

Culshaw, N. and Ketchum, J.
1995: The Kaipokok zone of the Makkovik orogen – an early Proterozoic terrane boundary? *In* Eastern Canada Shield Onshore-Offshore Transect (ECSOOT), Report of the 1994 Transect Meeting. *Complied by* R.J. Wardle and J. Hall. The University of British Columbia, Lithoprobe Secretariat, Lithoprobe Report 45, pages 7-21.

Davis, D.W.
1982: Optimum linear regression and error estimation applied to U–Pb data. Canadian Journal of Earth Sciences, Volume 19, pages 2141-2149.

Ermanovics, I.
1993: Geology of Hopedale Block, southern Nain Province, and the adjacent Proterozoic terranes, Labrador, Newfoundland. Geological Survey of Canada, Memoir No. 431, 161 pages.

1992: Geology, southern Hopedale Block, Labrador, Newfoundland; Geological Survey of Canada, Map 1669A, scale 1:100,000

Evans, D.
1980: Geology and petrochemistry of the Kitts and Michelin uranium deposits and related prospects, Central Mineral Belt, Labrador. Unpublished Ph.D. thesis, Queen's University, Kingston, Ontario, Canada, 311 pages.

Gandhi, S.S.
1978: Geological setting and genetic aspects of uranium occurrences in the Kaipokok Bay – Big River area, Labrador. Economic Geology, Volume 73, pages 1492-1522.

Gower, C.F., Flanagan, M.J., Kerr, A. and Bailey, D.G.
1982: Geology of the Kaipokok Bay–Big River area, Central Mineral Belt, Labrador. Newfoundland Department of Mines and Energy, Mineral Development Division, Report 82-7, 77 pages.

Hinchey, A.M.
2007: The Paleoproterozoic metavolcanic, metasedimentary and igneous rocks of the Aillik domain, Makkovik Province, Labrador (NTS map area 13O/03). *In* Current Research. Government of Newfoundland and Labrador, Department of Natural Resources, Geological Survey, Report 07-1, pages 25-44.

Hinchey, A.M. and LaFlamme, C.
2009: The Paleoproterozoic volcano-sedimentary rocks of the Aillik Group and associated plutonic suites of the Aillik domain, Makkovik Province, Labrador [NTS map area 13J/14]. *In* Current Research. Government of Newfoundland and Labrador, Department of Natural Resources, Geological Survey, Report 09-1, pages 159-182.

Hinchey, A.M. and Rayner, N.
2008: Timing constraints on the Paleoproterozoic, bimodal metavolcanic rocks of the Aillik Group, Aillik domain, Makkovik Province, Labrador. GAC-MAC 2008, Abstract Volume 33.

Kerr, A.
1994: Early Proterozoic magmatic suites of the eastern Central Mineral Belt (Makkovik Province), Labrador: geology, geochemistry and mineral potential. Government of Newfoundland and Labrador, Department of Natural Resources, Geological Survey, Report 94-03, 167 pages.

Kerr, A., Ryan, B., Gower, C.F. and Wardle, R.J.
1996: The Makkovik Province: extension of the Ketilidian Mobile Belt in mainland North America. *In* Precambrian Crustal Evolution in the North Atlantic Region. *Edited* by T.S. Brewer. Geological Society of London, Special Publication No. 1112, pages 155-177.

Kerr, A., Krogh, T.E., Corfu, F., Schärer, U., Gandhi, S.S. and Kwok, Y.Y.
1992: Episodic Early Proterozoic granitoid plutonism in the Makkovik Province, Labrador: U–Pb geochronological data and geological implications. Canadian Journal of Earth Sciences, Volume 29, pages 1166-1179.

Ketchum, J.W.F., Culshaw, N.G. and Barr, S.M.
2002: Anatomy and orogenic history of a Paleoproterozoic accretionary belt: the Makkovik Province, Labrador, Canada. Canadian Journal of Earth Sciences, Volume 39, pages 711-730.

Ketchum, J.W.F., Jackson, S.E., Culshaw, N.G. and Barr, S.M.
2001: Depositional and tectonic setting of the Paleoproterozoic Lower Aillik Group, Makkovik Province, Canada: evolution of a passive margin-foredeep sequence based on petrochemistry and U–Pb (TIMS and LAM-ICP-MS) geochronology. Precambrian Research, Volume 105, pages 331-356.

Krogh, T.E.
1982: Improved accuracy of U–Pb zircon ages by the creation of more concordant systems using an air abrasion technique. Geochimica et Cosmochimica Acta, Volume 46, pages 637-649.

Loveridge, W.D., Ermanovics, I.F. and Sullivan, R.W.
1987: U–Pb ages on zircon from the Maggo gneiss, the Kanairiktok Plutonic Suite, coast of Labrador, Newfoundland. Geological Survey of Canada, Paper 87-2, pages 59-65.

Marten, B.E.
1977: The relationship between the Aillik Group and the Hopedale gneiss, Kaipokok Bay, Labrador. Unpublished Ph.D. thesis, Memorial University of Newfoundland, St. John's, 389 pages.

Mattinson, J.M.
2005: Zircon U Pb chemical abrasion (CA-TIMS) method; combined annealing and multi-step partial dissolution analysis for improved precision and accuracy of zircon ages. Chemical Geology, Volume 220, pages 47-66.

Rivers, T., Ketchum. J., Indares, A. and Hynes, A.
2002: The high pressure belt in the Grenville Province: Architecture, timing, and exhumation. Canadian Journal of Earth Sciences, Volume 39, pages 867-893.

Ross, D.A.
2009: Technical report on the CMBNW property, Newfoundland and Labrador, Canada. NI 43-101 Technical Report, 101 pages.

Ryan, A.B.
1984: Regional geology of the central part of the Central Mineral Belt, Labrador. Newfoundland Department of Mines and Energy, Mineral Development Division, Memoir 3, 185 pages.

Schärer, U., Krogh, T.E., Wardle, R.J., Ryan, B. and Gandhi, S.S.
1988: U–Pb ages of early to middle Proterozoic volcanism and metamorphism in the Makkovik Orogen, Labrador. Canadian Journal of Earth Sciences, Volume 25, pages 1098-1107

Smyth, W.R., Marten, B.E. and Ryan, A.B.
1978: A major Aphebian-Helekian unconformity within the Central Mineral Belt of Labrador: Definition of new groups and metallogenic implications. Canadian Journal of Earth Sciences, pages 1954-1966.

Sparkes, G.W. and Dunning, G.R.
2009: Preliminary investigations into the style, setting and timing of uranium mineralization, Jacques Lake deposit, Central Mineral Belt, Labrador. *In* Current Research. Government of Newfoundland and Labrador, Department of Natural Resources, Geological Survey, Report 09-1, pages 81-93.

Sparkes, G.W., Dunning, G.R. and McNicoll, V.J.
2010: New U–Pb age constraints and potential implications for the genesis of the Kitts uranium deposit, Central Mineral Belt, Labrador. *In* Current Research. Government of Newfoundland and Labrador, Department of Natural Resources, Geological Survey, Report 10-1, pages 93-109.

Sparkes, G.W. and Kerr, A.
2008: Diverse styles of uranium mineralization in the Central Mineral Belt of Labrador: an overview and preliminary discussion. *In* Current Research. Government of Newfoundland and Labrador, Department of Natural Resources, Geological Survey, Report 08-1, pages 193-227.

Wardle, R.J. and Bailey, D.G.
1981: Early Proterozoic sequences in Labrador. *In* Proterozoic Basins of Canada. Geological Survey of Canada, Paper 81-10, pages 331-359.

Wardle, R.J., Gower, C.F., Ryan, B., Nunn, G.A.G., James, D.T. and Kerr, A.
1997: Geological Map of Labrador; 1:1 million scale. Government of Newfoundland and Labrador, Department of Mines and Energy, Geological Survey, Map 97-07.

Wilton, D.H.C
1996: Metallogeny of the Central Mineral Belt and adjacent Archean basement, Labrador. Government of Newfoundland and Labrador, Department of Mines and Energy, Geological Survey, Mineral Resources Report 8, 178 pages.

Wilton, D.H.C. and Longerich, H.P.
1993: Metallogenic significance of ICP-MS-derived trace element and Pb isotope data on uraninite separates from the Labrador Central Mineral Belt. Canadian Journal of Earth Sciences, Volume 30, pages 2352- 2365.